Oil Shale, 2013, Vol. 30, No. 2S, pp. 257–267
doi: 10.3176/oil.2013.2S.06
ISSN 0208-189X

INCREASING RENEWABLE FRACTION BY SMOOTHING CONSUMER POWER CHARTS IN GRID-CONNECTED WIND-SOLAR HYBRID SYSTEMS

ANDRES ANNUK[(a)*], ALO ALLIK[(a)], PRIIT PIKK[(a)], JAANUS UIGA[(a)], HEIKI TAMMOJA[(b)], KAUPO TOOM[(a)], JÜRI OLT[(a)]

[(a)] Institute of Technology, Estonian University of Life Sciences
Kreutzwaldi 56, 51014 Tartu, Estonia
[(b)] Department of Electrical Power Engineering, Tallinn University of Technology
Ehitajate tee 5, 19086 Tallinn, Estonia

Abstract. *Wind and solar irradiation are highly stochastic sources of energy. Nevertheless, to some degree, both are usable almost everywhere and are therefore very convenient energy sources. In the current paper, the performance of a small wind-photovoltaic (PV) panel hybrid system connected to the grid with or without storage equipment is estimated. The main purpose is to investigate possibilities of increasing the renewable fraction, which would reduce the need for electrical power from the grid, at different deviations of the unit consumer graph, while the yearly average consumption remains the same. The other important variable in calculations is battery size. Weather data is acquired from public meteorological databases.*

Keywords: *wind energy, solar energy, power chart, solar irradiation, consumer load, battery capacity, power limitation.*

1. Introduction

The pressure to increase the proportion of energy from renewable sources in final energy consumption has been growing in the last years. According to Directive 2009/28/EC of the European Parliament and of the Council of 23 April 2009 on the promotion of the use of energy from renewable sources, all EU Member States are obliged to increase the share of renewables in final energy consumption by 2020 compared to the reference year 2005. Estonia has to achieve a 25% target for the share of energy from renewable sources by 2020 as against 18% in 2005 [1].

* Corresponding author: e-mail *andres.annuk@emu.ee*

Several sources of energy (biomass, wind power, solar radiation and ground heating) could be used to achieve the target set. Being easily available, wind and solar radiation are convenient sources of energy. However, the main problem is the very high stochastic nature of wind and solar energy.

It is characteristic of the wind energy generator equipment that its energy payback period is shortest (less than 0.5 year) compared to other energy generating technologies [2].

The amount of installed wind energy generating capacities is increasing rapidly; therefore it is necessary to develop balancing capabilities for wind power capacities connected to the grid. For example, the operating variables of today's oil shale-based power plants are not meant for balancing the rapidly changing stochastic electrical power inputs to the grid [3]. In the near future, the development of wind capacities will exceed the balancing possibilities currently available in the grid. The best way to balance wind power units would be to use hydropower stations. Unfortunately, the utilization of hydropower as a balancing element is mostly limited due to the lack of available necessary capacities for several reasons. The exploitation of energy system resources of neighbouring countries is restricted as well, because most countries are already engaged in developing wind power.

Another opportunity for reducing the effect of a wind generator on the grid is a combined production of wind-PV energy. Solar energy is becoming more competitive due to the continuously decreasing prices for PV panels [4]. Owners of wind and PV units are interested in selling more energy to the grid and purchasing as small quantities of energy from the grid as possible. Research shows that the amount of energy to be obtained from the grid is minimal if the ratio of wind to PV power is 70:30 [5, 6]. This shows that wind and PV units have certain balancing properties when operating together. The need for storage equipment is determined by the characteristic consumption distribution in time. Some storage elements are probably needed in the system to maintain control over energy flows.

The goal of this paper is to evaluate possibilities for diminishing the amount of energy purchased from the grid in case of different standard deviations of the unit consumer graph by using various accumulation capacities.

2. Wind-PV system architecture

In the current article, the efficiency of a grid-connected integrated renewable system consisting of a consumer, wind generators, PV panels, a DC/AC inverter and storage devices (Fig. 1) is assessed. Primary data processing was implemented by Microsoft Excel and Homer (Homer Energy, US) software. One regular year of 8760 hours that includes all seasons served as an evaluation period. The amount of energy received from the grid was limited in a way that the capacity shortage would not exceed 0.1%. At the

same time, the size of the wind and PV energy generation equipment was chosen so that the above-mentioned 70:30 ratio could be adhered to.

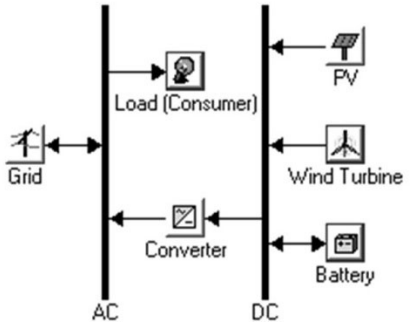

Fig. 1. Block diagram of the system architecture.

3. Consumer load analysis

The annual electricity consumption data was synthesised from measurements made in a typical Estonian rural dwelling house during one week in February and one week in August. Characteristic of this data is that the density and amplitude of peak loads are higher in summer than in winter. The reason for this is that the equipment employed in rural households in the summertime is mainly used for water pumping, firewood cutting, etc., and therefore the consumption of maximal electrical power in summer is higher whereas the base load electricity consumption is higher in winter because there is a higher need for lighting and other daily applications during this time of the year.

The load profile of the hourly average of one week in winter (beginning on Monday 4th February 2008) is shown in Figure 2. Figure 3 illustrates the load profile of a summer week (beginning on Monday 28th July 2008). The base load occurs from 1 am until 7 am, whereas the majority of the load falls on evening hours (from 16 pm to 1 am).

As can be seen from Figures 2 and 3, minimum and maximum loads during all periods are 0.098 and 3.51 kW, respectively. The random variability of the consumption graph in the sequence of daily averages is 25.5% and the difference between hourly energy consumption data and average daily energy usage profile is 57% according to formulas utilized by Homer software [7]. This is a sufficiently fluctuating chart to represent the majority of consumer profiles.

Standard deviation was found from annual power consumption data that was synthesized from the weekly power consumption. Since the standard deviation of consumption data in the sequence of daily averages, as a difference between hourly data and average daily profile, is used to assess the unit consumer chart, it is reasonable to use the standard deviation δ for

assessing the whole chart [8]. In the current case, δ = 0.76 kW. As the average power consumption P_C = 1 kW, the above-mentioned standard deviation also characterizes the relative standard deviation. In order to examine different consumer charts, i.e. sharply or gently sloping ones, the variation from the average value (P_c) is altered. For this Equation (1) is used:

$$P_\delta = P_C + (P_{mean} - P_C) \cdot \delta \,, \tag{1}$$

where P_δ is the altered-dispersion power consumption by a unit consumer, kW;
P_C is the power consumption by a unit consumer with 1 kW average, kW;
P_{mean} is the average power consumption by a unit consumer.

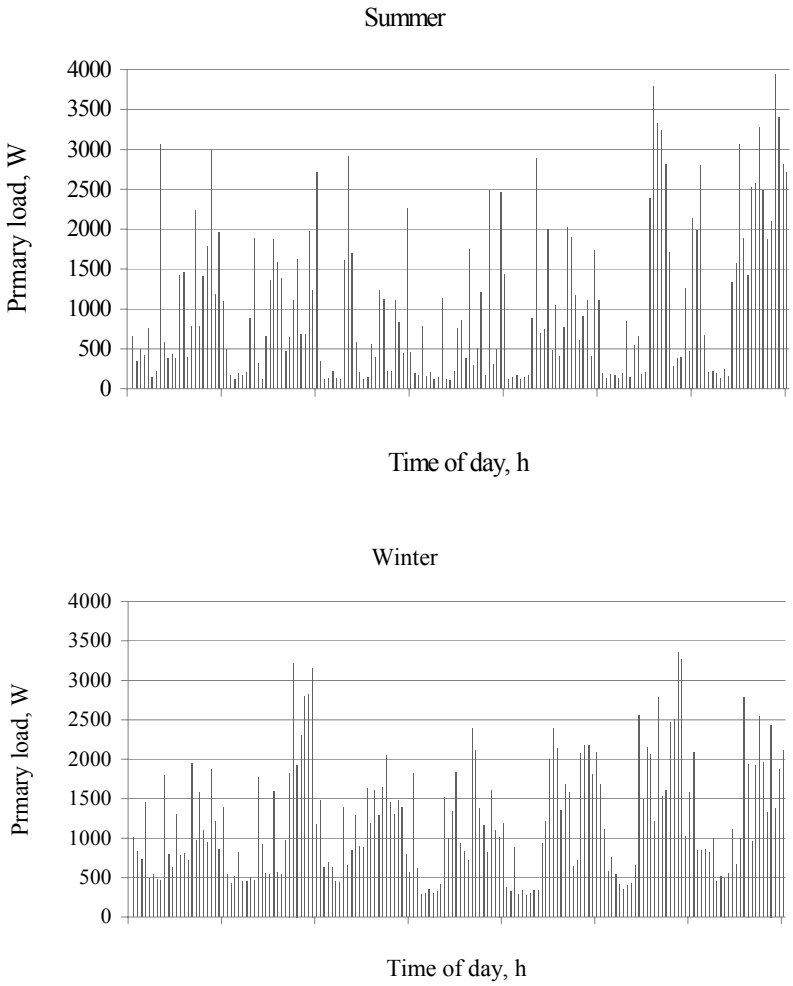

Fig. 2. Weekly load profile in summer and winter.

4. Global solar irradiation and wind speed data

Calculations were based on averaged hourly wind speed and global irradiation data measured by the Estonian Meteorological and Hydrological Institute (EMHI) in Estonian locations of Tõravere and Tiirikoja in 2004–2009.

The solar irradiation data measured in one location, Tõravere, was used on a suggestion that in the territory of Estonia, the annual actinometrical resource varies, reaching 5.5%, which corresponds to 890–990 kWh/m^2/year [9]. The data from Tõravere was used as it describes quite precisely the average global solar irradiation in Estonia.

In Figure 3 solar irradiation data measured at Tõravere in the sample year 2008 is presented. It can be seen that in wintertime, this actinometrical solar irradiation resource is uneconomical for producing household electricity, especially from December to January. In February and March the amount of solar radiation increases because of less cloud coverage and more diffused radiation reflected from snow. The ratio of direct to diffused radiation in winter months is 0.2–0.6, while in summer months it falls in the range of 0.6–1.2 [5, 10]. The efficiency of a PV panel system under standard test conditions is assumed to be 12%.

The most commonly recommended PV array angle is equal to the latitude because this provides the most even production chart throughout the year [9, 11]. Taking into consideration the opening of the electricity market in 2013 and for increasing the renewable fraction in own consumption, it will be reasonable to produce as much energy as possible in colder seasons.

To calculate the best angle of the tilt in the winter season (from October until March), the latitude is multiplied by 0.89 and 24 degrees are added [11]. The latitude of the measuring point is 58.26° and according to the above data, an optimal tilt angle from the horizontal for winter conditions is 75.85°.

In this paper, the derating factor f_{PV} = 90% [12] is used for panels without a tracking system; therefore the panels have an azimuth of 0 degree to south.

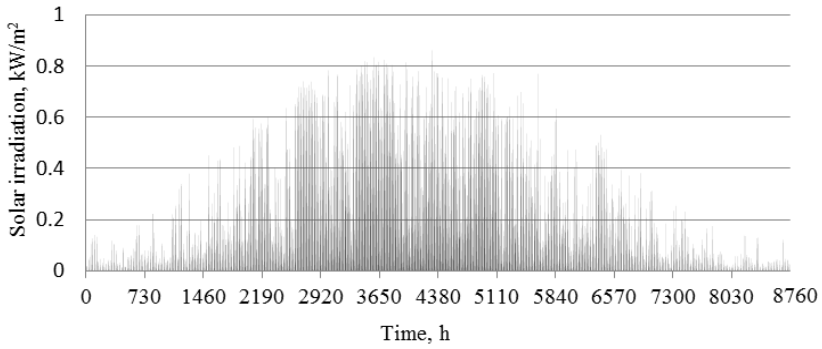

Fig. 3. Solar irradiation data measured at Tõravere in 2008 (according to EMHI).

To calculate the output of the PV panel the following equation is used [7]:

$$P_V = Y_{PV} f_{PV} \frac{\overline{G}_T}{\overline{G}_{T,STC}} [1 + \alpha_P (T_c - T_{c,STC}], \quad (2)$$

where Y_{PV} is the rated capacity of the PV array power output under standard test conditions, kW;

f_{PV} is the degrading factor of PV, %;

$\overline{G}_T$ is the solar radiation incident on the PV array in the current time step, kW/m^2;

$\overline{G}_{T,STC}$ is the incident radiation under standard test conditions, 1 kW/m^2;

a_P is the temperature coefficient of power, %/°C;

T_c is the temperature of the PV cell in the current time step, °C;

$T_{c,STC}$ is the temperature of the PV cell under standard test conditions, 25 °C.

The power output of the wind turbine is calculated every hour. This entails a two-step process. First, the wind speed at the hub height of the wind turbine is calculated, then the amount of power the wind turbine would produce at a certain averaged hourly wind speed is found.

By using wind speed hourly averaged data the Weibull shape factor k in different locations on the territory of Estonia was analyzed. The wind speed data used was measured at the height of 10 m from the surrounding surface, which in our study was around 90 m above sea level. From the database it was calculated that the average k = 1.77 with a relative standard deviation δ = 0.06. The database consists of 30 time series of 6 years (2004–2009) and 5 different places (coastal and inland regions), namely Tiirikoja, Jõgeva, Pakri, Tõravere, and Viljandi. Although in these locations the Weibull shape factor values for wind speed are rather similar, the case is different for other locations in Estonia. For example, at Virtsu and Sõrve, the shape factor k is considerably higher, reaching as high as 2. The wind data of Tiirikoja (Fig. 4) of the year 2006 is used because this year's Weibull shape factor k = 1.77.

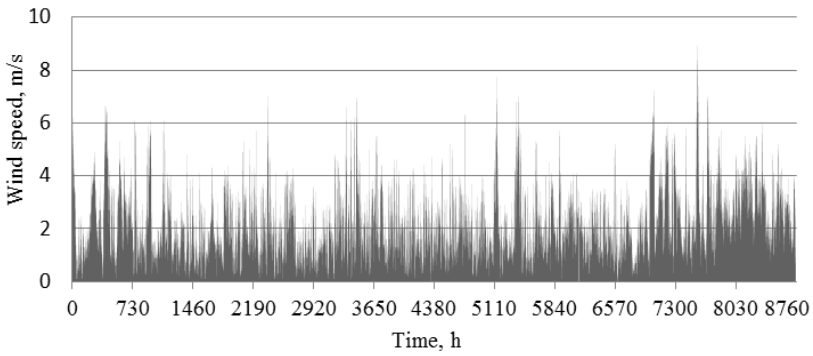

Fig. 4. Wind speed hourly data measured at Tiirikoja, 2006.

The power curve (3) of a wind generator is averaged from those of several wind generators that are most suitable for moderate wind conditions. It should also be noted that this normalized power curve has the following limiters. If the wind speed $v < 2.5$ m/s, $P = 0$ kW, and when $v > 12$ m/s, $P = 1$ kW [13]:

$$P = 0.0078 \cdot v^2 - 0.0229 \cdot v + 0.00866022, \tag{3}$$

where v is the hourly averaged wind speed, m/s;
P is the output power, kW.

The hub height of 30 m was chosen. To transform wind speed data to the chosen height, 30 m, a logarithmic relation was used. The surface roughness $z_0 = 0.25$ was used since it is characteristic of the landscape in rural areas, with many trees but few buildings.

5. Parameters of the inverter and storage device

A DC/AC inverter with a nominal power of 10 kW and efficiency of 90% is used. Losses in the inverter are around 900 kWh per year. Sealed deep-cycle lead-acid batteries with a minimal state of charge SOC = 40% and capacity of 200 Ah, i.e. useable 1.44 kWh and roundtrip efficiency of 80%, are employed as storage device. The batteries are connected to strings by four pieces, with a total output voltage of 48 V.

6. The energy balance of the system

The energy balance of the hybrid system shown in Figure 1 is the following:

$$W_C = W_W + W_{PV} + W_G - W_{Bl} - W_{GS} - W_{Il}, \tag{4}$$

where W_C is the energy consumption by a unit consumer, kWh/year;
W_W is the amount of energy produced by wind generators, kWh/year;
W_{PV} is the amount of energy produced by PV arrays, kWh/year;
W_{Gp} is the amount of energy purchased from the grid, kWh/year;
W_{Bl} is the energy loss in the battery, kWh/year;
W_{Il} is the energy loss in the inverter, kWh/year;
W_{Gf} is the amount of energy fed to the grid, kWh/year.

A unit consumer's average power demand is 1 kW, which means a 8760 kWh consumption per year. The capacity factors are respectively solar and wind devices $CF_S = 0.084$ and $CF_W = 0.115$. These factors remain constant during the study, but the capacities change. To cover losses in the storage equipment, wiring and the inverter, we suggest using enough wind generators and PV arrays to cover at least:

$$W_W + W_{PV} \rightarrow 10000 \text{ kWh/year} \tag{5}$$

It should be noted that the average capacity of renewable energy sources must be tightly tied with consumption in order to avoid extensive over-production. In order to comply with prequisite (5) in the wind and solar conditions chosen, the 7 kW wind generator and PV panels with a total power of 4.12 kW are used.

7. Renewable fraction of the total electrical energy produced

As follows, possibilities of increasing the renewable fraction for different standard deviations of the consumer chart are investigated. The power obtained from the grid, P_L, is limited (capacity shortage $C_S < 0.1\%$) and the number of batteries is correspondingly increased. Table 1 presents the results when the standard deviation $\delta = 0.76$ kW.

W_T is the total energy received from the wind generator, PV panels and the grid (6):

$$W_T = W_W + W_{PV} + W_{Gp} \tag{6}$$

The renewable fraction W_R is calculated by using the following formula:

$$W_R = \frac{W_{PV} + W_W}{W_T} \tag{7}$$

It can be seen from Table 1 that adding batteries increases the renewable fraction W_R, reduces the need for energy from the grid W_{Gp} and reduces the amount of energy fed to the grid W_{Gf}. When the capacity of batteries is increased further, the above effect will diminish, while losses in the batteries are reduced as well. The correlations presented in Table 1 are illustrated in Figure 5.

The escalation of the renewable fraction by adding batteries is linear until 23.0 kWh. At the same time, the power received from the grid is reduced to a value which is smaller than that of power fed to the grid.

Table 1. Parameters of the system with $\delta = 0.76$ kW

Battery capacity, W_B, kWh	Energy from the grid, W_{Gp}, kWh	Total energy received, W_T, kWh	Energy fed to the grid, W_{Gf}, kWh	Maximal power from the grid, P_L, kW	Renewable fraction, W_R	W_{Bl}, kWh
0	4803	14843	5079	0	0.676	1004
5.76	4524	14564	4731	2.5	0.689	996
11.52	4257	14297	4397	2.4	0.702	989
17.28	3945	13984	4010	2.2	0.718	983
23.04	3637	13676	3628	2	0.734	972
28.8	3470	13509	3421	1.9	0.743	967
34.56	3423	13462	3360	1.9	0.746	966
40.32	3392	13431	3319	1.9	0.747	965

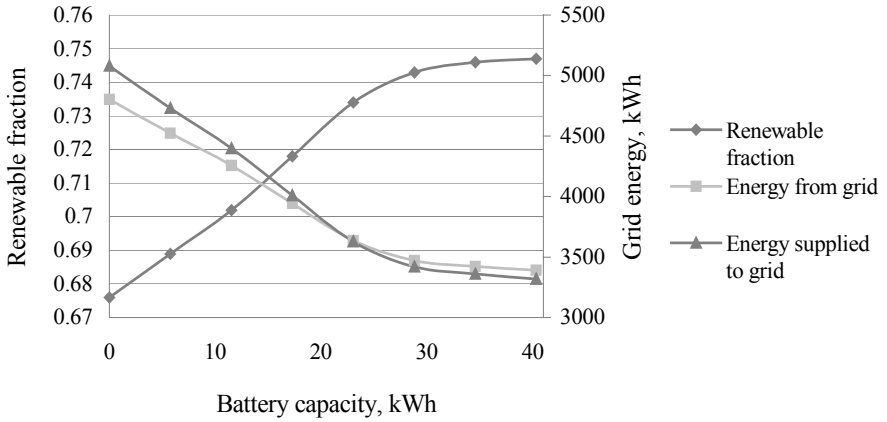

Fig 5. Dependence of renewable fraction and energy from and to the grid on battery capacity, with a maximum consumption dispersion of 0.76 kW.

The consumer chart shown in Figure 6 describes the change of the renewable fraction at different standard deviations and variable amounts of battery capacities. It can be seen that if the standard deviation is increaced without adding any batteries to the system, the renewable fraction is reduced. When batteries are added, the renewable fraction starts increacing and reaches a maximal value W_R = 0.779 when δ = 0.25 ± 0.05 kW. Adding batteries with a total accumulation capacity over 23 kWh does not remarkably increace the renewable fraction.

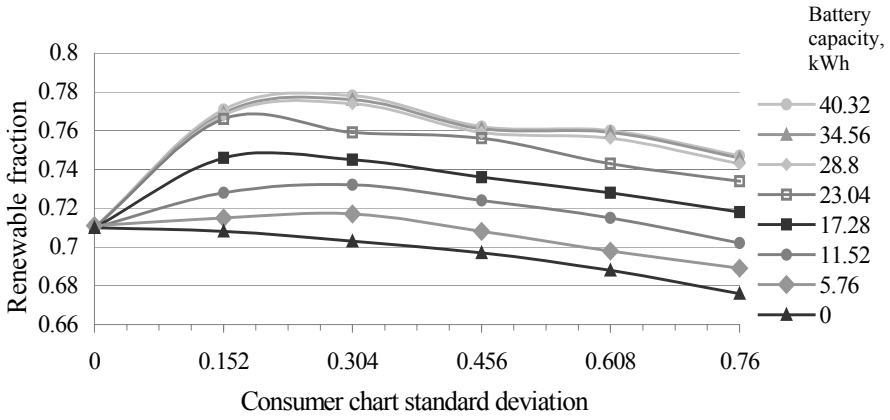

Fig 6. Influence of battery capacity on renewable fraction at different standard deviation values of the consumption curve.

8. Conclusions

In the current article, possibilities for increasing the grid-connected wind-PV system's renewable fraction (ratio of energy produced from wind and solar radiation to total energy obtained, i.e. energy from the grid), reducing the amount of energy received from the grid as a result, were investigated. A unit consumer with an average power consumption of 1 kW was used for assessing the efficiency of the system. The unit consumer was created by reducing the actually measured consumption of power by a consumer. Different standard deviation charts were created from this unit consumer chart. The most representative wind and solar data was used. The methology used in this research can be used for the development of real wind-PV systems connected to the grid by using smart-grid solutions.

On the basis of the results presented above, the following conclusions can be drawn:

1. In case of grid-connected wind-PV systems without batteries the renewable fraction exhibits a decreasing trend with increasing standard deviation of the consumption curve.
2. When batteries are added to the grid-connected wind-PV system, the renewable fraction is the highest at the standard deviation $\delta = 0.25 \pm 0.05$ kW of the consumption curve. If this value is higher or lower, the renewable fraction decreases. Therefore the consumption curve should not be too flat.
3. If the standard deviation $\delta = 0$, the battery capacity has no influence on the renewable fraction.

REFERENCES

1. Directive 2009/28/EC of the European Parliament and of the Council. *Official Journal of the European Union*. 2009, L 140/16. P. 46. Available at http://eur-lex.europa.eu/LexUriServ/LexUriServ.do?uri=OJ:L:2009:140:0016:0062:en:PDF (03.11.2011).
2. Mathew, S. *Wind Energy: Fundamentals, Resource Analysis and Economics*. Springer, Berlin, 2006.
3. Palu, I., Oidram, R., Keel, M., Tammoja, H. Balancing of wind energy using oil-shale based power plants at erroneous wind forecast conditions. *Oil Shale*, 2009, **26**(3S), 189–199.
4. Wilkinson, S. PV module costs and prices: what is really happening now? *Inter PV. 2010*. Available at http://www.interpv.net/wsr/wsr_view.asp?idx=252&part_code =01&page=4 (03.11.2011). http://www.pv-tech.org/guest_blog/pv_module_costs_and_prices_what_is_really_happening_now_5478
5. Annuk, A., Pikk, P., Kokin, E., Karapidakis, E. S., Tamm, T. Performance of wind-solar integrated grid connected energy system. *Agronomy Research*, 2011, **9**(1–2), 273–281.

6. Caralis, G., Delikaraoglu, S., Zervos, A. Towards the optimum mix between wind and PV capacity in the Greek power system. *European Wind Energy Conference & Exhibition Scientific Proceedings*, 2011, 75–79.
7. *Homer Energy*. Available at http://homerenergy.com/ (05.11.2011).
8. Meldorf, M. *Electrical Network Load Monitoring*. TUT Press, Tallinn, 2008.
9. Tomson, T. *Helio Energetics – Technical Use of Solar Energy*. Humare, Tallinn, 2000 (in Estonian).
10. Russak, V., Kallis, A. *Handbook of Estonian Solar Radiation Climate*. Estonian Meteorological and Hydrological Institute (EMHI), Iloprint, Tallinn, 2003 (in Estonian).
11. Rowlands, I. H., Kemery, B. P., Beausoleil-Morrison, I. Optimal solar-PV tilt angle and azimuth: An Ontario (Canada) case-study. *Energ. Policy*, 2011, **39**(3), 1397–1409.
12. Al-Karaghouli, A., Kazmerski, L., L. Optimization and life-cycle cost of health clinic PV system for a rural area in southern Iraq using HOMER software. *Sol. Energy*, 2010, **84**(4), 710–714.
13. Põder, V., Lepa, J., Palge, V., Peets, T., Annuk, A. The estimation of needed capacity of a storage system according to load and wind parameters. *Oil Shale*, 2009, **26**(3S), 283–293.

Received October 24, 2012